ISSN 1070-3632, Russian Journal of General Chemistry, 2020, Vol. 90, No. 8, pp. 1533–1543. © Pleiades Publishing, Ltd., 2020.

A Swift One-Pot Solvent-Free Synthesis of Benzimidazole Derivatives and Their Metal Complexes: Hydrothermal Treatment, Enzymatic Inhibition, and Solubilization Studies

M. B. Taj[a,b,*], A. Raheel[c], W. Alelwani[d], D. Hajjar[d], A. Makki[d], A. M. Alnajeebi[d], N. A. Babteen[d], S. A. Tırmizi[c], and S. Noor[e,]**

[a] *Department of Chemistry, Islamia University, Bahawalpur, 63100 Pakistan*
[b] *Department of Chemistry, University of Sahiwal, Sahiwal, 57000 Pakistan*
[c] *Department of Chemistry, Quaid-e-Azam University, Islamabad, 44000 Pakistan*
[d] *Department of Biochemistry, College of Science, University of Jeddah, Jeddah, 80203 Saudi Arabia*
[e] *Department of Chemistry, University of Agriculture, Faisalabad, 38000 Pakistan*
*e-mail: *drbabartaj@gmail.com; **sadiaa613@gmail.com*

Received May 31, 2020; revised July 20, 2020; accepted August 5, 2020

Abstract—Three benzimidazole derivatives, 1-(1*H*-benzimidazol-2-yl)ethanol (HBE), 1*H*-benzimidazol-2-yl(diphenyl)methanol (BDM) and 1,2-bis(1*H*-benzimidazol-2-yl)ethane-1,2-diol (BHBED), have been synthesized following the one-pot rapid green protocol. Complexes of benzimidazole derivatives with six 3*d* transition metals, Cu(II), Mn(II), Zn(II), Fe(II), Co(II), and Ni(II), have been synthesized by free hydrothermal method. The synthesized products have been characterized by FTIR, ^{1}H, and ^{13}C NMR, and mass spectroscopy, and CHN analysis, and 2:1 ligand to metal stoichiometry has been confirmed. The synthesized ligands and metal complexes have been tested for antioxidant potential (DPPH), inhibitory activity including inhibition of acetylcholinesterase (AChE), butyrylcholinesterase (BChE), lipoxygenase (LOX), α-glucosidase. Micellar solubilization of the metal complexes has been studied in sodium dodecyl sulphate (SDS) by UV-Vis spectroscopy and conductivity. The selected complexes of nickel, zinc and cobalt have demonstrated interaction with SDS, and the value of critical micellar concentration increased in all cases.

Keywords: anionic surfactant, benzimidazole derivatives, hydrothermal treatment, inhibition activity, micellar solubilization, 3*d* metal complexation

DOI: 10.1134/S107036322008023X

INTRODUCTION

Benzimidazole drivatives have been explored as poisons in non-nucleoside topoisomerase-I and inhibitors of reverse transcriptase against HIV-1 and DNA-gyrase [1]. Benzimidazoles can act as ligands in binding with transition metals for experimental modelling in the biological systems [2–4]. Numerous routes to their synthesis, including the coupling of *o*-phenylenediamines with carboxylic acids [5], aldehydes [6] and *o*-esters under catalysis by Lewis acids [7] are reported. Phthalic acid attached to polymer-supported 4-fluoro-3-nitrobenzoic acid and polyethylene glycol ether in solid phase has been reported as a precursor for 2-substituted benzimidazoles, benzoxazoles and benzothiazoles [8]. High selectivity of transition metals, especially 3*d*, 4*d*, and 5*d*, stimulated studies of their complexes biological and enzymatic activities [9]. However, synthetic approaches to such compounds are retarded by stringent reaction conditions, multistep procedures, low yields, and unavoidable side reactions. Therefore, search for efficient synthetic approaches to such compounds is still of considerable importance.

The structural similarities of micelles and biological membranes allow the former ones to be used as substitute models for *in vitro* study of drug-membrane interactions [10–14]. Some valuable information on solubilization of transition metal complexes with nitrogen-donor ligands has been presented [15–19].

Herein, we present the green one-pot solvent-free synthesis of benzimidazole derivatives, their complexation with different 3d metals and some biological properties.

Scheme 1.

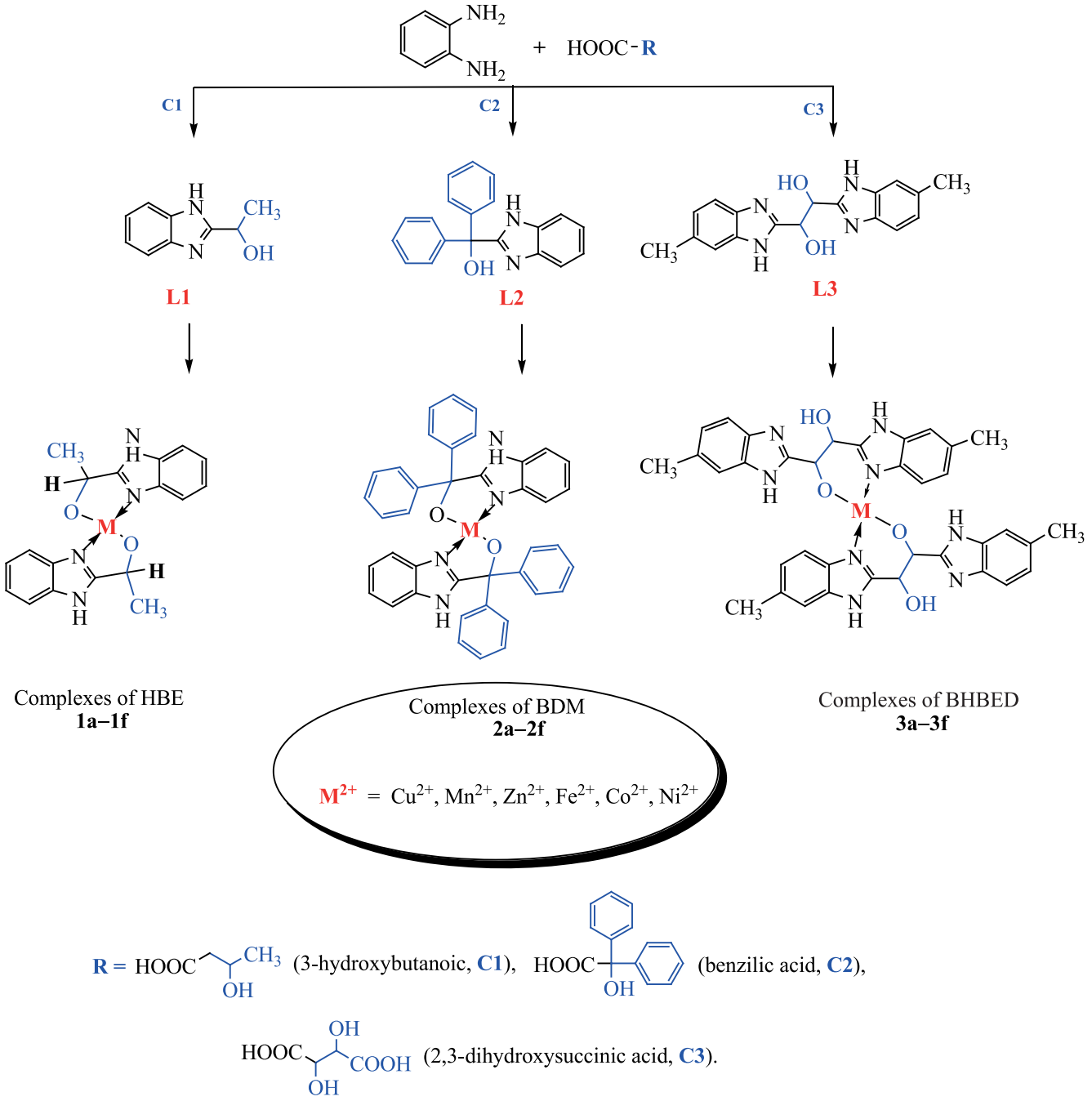

RESULTS AND DISCUSSION

The pure ligands **L1**–**L3** were synthesized by a highly efficient one-pot solvent-free method (Scheme 1). Their structural and physical characteristics were in close agreement with those reported for the known compounds.

FTIR spectra confirmed formation of the ligands and their complexes. The doublet of NH_2 at 3450 cm^{-1} in the spectrum of *o*-phenylenediamine was not recorded because of proton removal from the amino group of ligands as confirmed by the presence of singlets at 3350, 3360, and 3360 cm^{-1} for HBE, BDM, and BHBED, respectively. Formation of ligands was confirmed by C–N peaks at 1655, 1630, and 1630 cm^{-1}, respectively. The bands of O–H were not recorded in the spectra of complexes indicating involvement of oxygen in the complexation. The bands of C–N of the complexes were

Table 1. Biological activities of the synthesized ligands and their complexes

DPPH Radical Scavenging activity							
Sample	Ligand–complex	Inhibition, %	IC_{50}	Sample	Ligand–complex	Inhibition, %	IC_{50}
L1	HBE	87.02±0.71	104.11±0.11	**2c**	$(BDM)_2Zn$	72.89±0.11	208.91±0.41
1d	$(HBE)_2Fe$	85.23±0.25	81.71±0.18		Control	Quercetin	16.96±0.14
1e	$(HBE)_2Co$	86.85±0.62	141.81±0.16				
Acetylcholinesterase (AChE) inhibition activity							
L1	HBE	61.81±0.71	192.61±0.21	**2b**	$(BDM)_2Mn$	41.71±0.18	423.11±0.15
L2	BDM	56.45±0.65	212.61±0.71	**2d**	$(BDM)_2Fe$	53.60±0.32	427.31±0.1
1a	$(HBE)_2Cu$	51.93±0.45	423.11±0.32	**2f**	$(BDM)_2Ni$	77.34±0.34	145.71±0.11
1c	$(HBE)_2Zn$	41.71±0.18	423.11±0.15	**3b**	$(BHBED)_2Mn$	55.61±0.01	409.11±0.14
1f	$(HBE)_2Ni$	70.63±0.44	183.51±0.34		Control	Eserine	0.04±0.01
2a	$(BDM)_2Cu$	56.11±0.25	212.91±0.33				
Butyrylcholinesterase (BChE) inhibition activity							
1f	$(HBE)_2Ni$	64.61±0.11	238.21±0.44	**3c**	$(BHBED)_2Zn$	82.09±0.31	186.51±0.05
2f	$(BDM)_2Ni$	60.50±0.21	278.91±0.34		Control	Eserine	0.85±0.001
Lipoxygenase (LOX) inhibition activity							
L3	BHBED	53.71±0.35	412.31±0.11	**3e**	$(BHBED)_2Co$	49.24±0.41	–
1b	$(HBE)_2Mn$	59.89±0.1	376.11±0.58	**3f**	$(BHBED)_2Ni$	29.30±0.34	–
3d	$(BHBED)_2Fe$	51.86±0.28	<400		Control	Baicalein	22.4±1.3
α-Glucosidase activity							
2c	$(BDM)_2Zn$	70.49±0.82	134.20±0.25		Control	Acarbose	36.20±0.05
3c	$(BHBED)_2Zn$	81.33±0.98	244.57±0.74				
Anti-urease activity							
1c	$(HBE)_2Zn$	77.79±0.82	61.34±0.25	**3b**	$(BHBED)_2Mn$	86.12±0.98	244.57±0.74
2c	$(BDM)_2Zn$	75.49±0.84	134.3±60.56		Control	Acarbose	21.25±0.15

recorded in lower field region 1429–1547 cm^{-1} than those of the ligands (1655–1630 cm^{-1}).

^1H NMR and mass spectra clearly supported formation of the ligands and their corresponding complexes.

Biological tests of the synthesized compounds. The ligands and their metal complexes were screened for biological activities including antioxidant DPPH activity, inhibition of acetylcholinesterase (AChE), butyrylcholinesterase (BChE), lipoxygenase (LOX), α-glucosidase, and urease [20–27]. According to the initial biological tests, the metal complexes demonstrated higher biological potential than their ligands due to availability of metal-ligand bond for the corresponding processes of inhibition (Table 1).

The ligand HBE and its complexes with iron, cobolt and nickel were characterized by the highest antioxidant potential in DPPH radical scavenging assay. In the case of acetylcholinesterase (AChE) inhibition, the complexes $(HBE)_2Cu$, $(BDM)_2Mn$ and $(BHBED)_2Mn$ exhibited the highest activity as compared to other counterparts. In terms of butyrylcholinesterase (BChE) inhibition, the complexes $(HBE)_2Ni$, $(BDM)_2Ni$ and $(BHBED)_2Zn$ were characterized by the higher inhibition activity than the other complexes and ligands. The complex $(HBE)_2Mn$ and the complexes of ligand BHBED with Fe, Co and Ni were the most potent inhibitors of lipoxygenase (LOX). The highest α-glucosidase activity was determined for the complexes $(BDM)_2Zn$, $BHBED)_2Mn$ and $BHBED)_2Zn$, whereas promising results of anti-urease activity were achieved with the complexes $(HBE)_2Zn$, $(BDM)_2Zn$ and $(BHBED)_2Mn$.

Electrical conductivity. Values of CMC (critical micellar concentration) and other thermodynamic parameters were studied in the presence of metal complexes in the micellar media. Gradual dilution led to noticeable changes in the conductivity. The effect of temperature changes on micellization and CMC of surfactants on its interaction with metal complexes was tested (Fig. 1). The CMC was calculated at the intersection of two straight lines in the plots [15–19, 28–31]. The presence of metal complexes led to an increment in CMC with increasing temperature of the medium.

The thermodynamic parameters summarized in Table 2 clearly indicated the significant interaction between

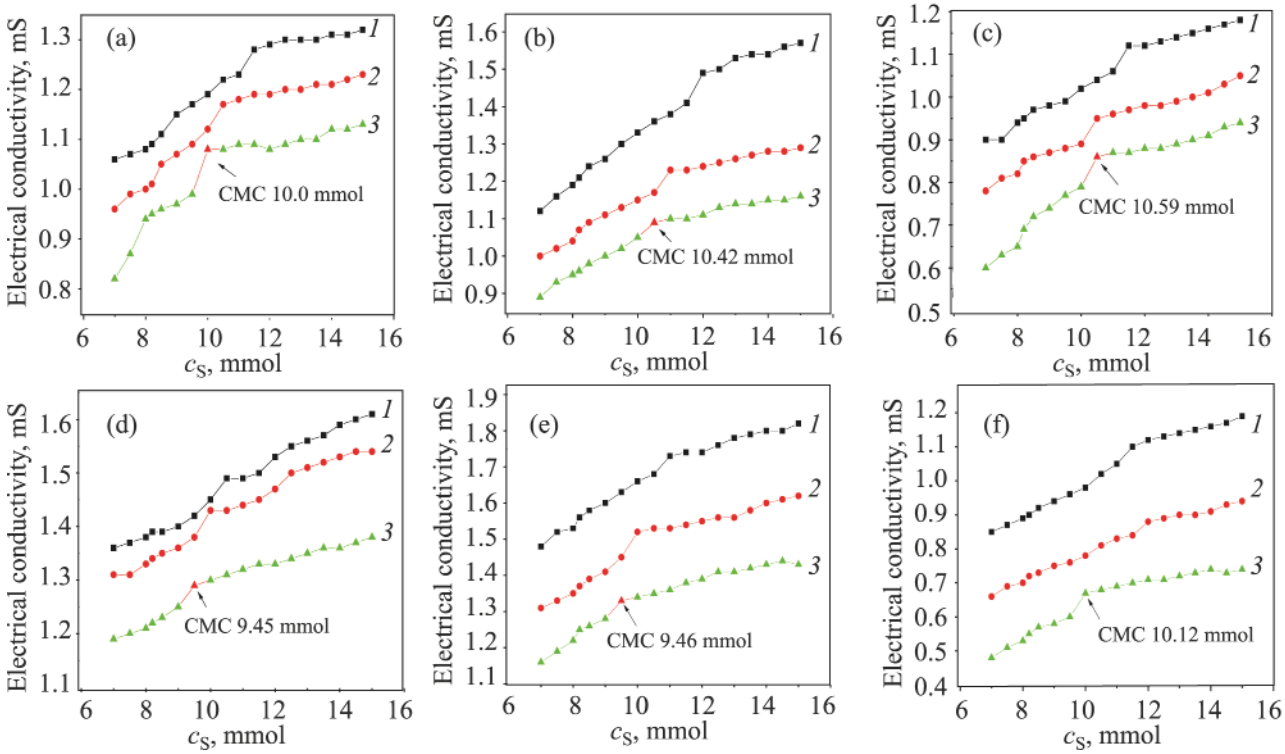

Fig. 1. Graphical representation of electrical conductivity at various temperatures [(*1*) 45, (*2*) 35, (*3*) 25°C]. (a) $(HBE)_2Ni$, (b) $(BDM)_2Ni$, (c) $(BHBED)_2Ni$, (d) $(BDM)_2Zn$, (e) $(BHBED)_2Zn$, and (a) $(HBE)_2Co$.

complex and micelles of SDS at different temperatures. The process was entropy-driven as confirmed by the positive values of ΔS_m due to transfer of hydrophobic tails to core micellar region from aqueous medium. Significant hydrogen bonding around the non-polar tail ends differentiated hydrophobic hydration and conventional solute-solvent interactions [15–19]. Screening of metal complexes (1.5 mmol) [$(HBE)_2Ni$; $(BDM)_2Ni$; $(BHBED)_2Ni$; $(BDM)_2Zn$; $(BHBED)_2Zn$; $[(HBE)_2Co]$ was carried out at the micellar concentration of SDS equal to 8.2 mmol. The similar trend was observed in the study of UV-Vis absorbance (Table 2).

UV-Vis spectra. Interaction of metal complexes with surfactant SDS was studied by UV-Vis spectroscopy and its differential version. The values of λ_{max} of aqueous solutions of complexes were recorded in the presence and absence of the surfactant and then plotted against the concentration of SDS (Fig. 2). The extent of interaction of complexes with SDS was assessed by the shift of λ_{max} in the spectra. It was speculated that the prevalence of electrostatic and hydrophobic interactions could cause incorporation of molecules of metal complexes in the proximity of micelles of SDS. The value of absorbance gradually increased upon the increase of concentration of SDS due to gradual incorporation of the complex within micelles, and the critical micellar concentration increased in all cases. The bathochromic shift indicated interaction and association of nickel complexes with the surfactant [15–19].

The actual starting point of micellization was hard to standardize but this change could be measured by means of some physical parameters such as UV-Vis absorbance, electrical conductivity, surface tension, light scattering, and solubilization. These physical properties could be used for approximating the value of CMC [9–19, 28–31] (Table 3).

Increase of differential absorption was growing with SDS concentration and indicated constant incorporation of metal complex molecules in the micellar system. In the presence of $(HBE)_2Ni$ the CMCs of SDS shifted from 8.2 to 10.1 mmol, similarly $(BDM)_2Ni$ increased CMC to 10.51 mmol, $(BHBED)_2Ni$ to 10.57 mmol; $(BDM)_2Zn$ to 9.26 mmol; $(BHBED)_2Zn$ to 9.55 mol, and $(HBE)_2Co$ to 10.03 mmol. Penetration of metal complexes into SDS micelles led to higher values of CMC in comparison with pure SDS.

The intermolecular hydrogen bond between the units of metal complexes and water molecules led to adsorption

Table 2. Micellar and thermodynamic parameters determined for the selected metal complex in SDS

Complex	T, °C	CMC, mmol	ΔG_m, kJ/mol	ΔH_m, kJ/mol	ΔS_m, J mol^{-1} K^{-1}	β
$(HBE)_2Ni$	25	10.00	–39.814	–3.49	121.91	0.14
	35	10.55	–39.962	–3.61	118.04	0.19
	45	11.53	–40.473	–3.88	115.07	0.18
$(BDM)_2Ni$	25	10.42	–36.116	–9.98	88.24	0.30
	35	11.02	–35.568	–10.40	81.74	0.32
	45	12.16	–37.491	–10.70	84.16	0.37
$(BHBED)_2Ni$	25	10.59	–37.060	–5.35	106.43	0.25
	35	10.51	–33.010	–5.10	90.62	0.44
	45	11.53	–34.940	–5.24	93.40	0.5
$(BDM)_2Zn$	25	9.45	–34.420	–5.99	95.40	0.40
	35	10.01	–24.330	–5.11	62.39	0.72
	45	10.46	–29.020	–4.70	76.49	0.90
$(BHBED)_2Zn$	25	9.52	–36.350	–3.16	1011.36	0.31
	35	9.96	–35.310	–3.27	104.04	0.36
	45	11.00	–35.870	–3.40	105.26	0.40
$(HBE)_2Co$	25	10.12	–37.730	–11.40	88.26	0.23
	35	11.98	–35.070	–10.40	79.97	0.49
	45	12.04	–33.760	–11.90	68.61	0.38

Table 3. Solubilization parameters for selected metal complex in the micellar media of SDS

Complex	K_x, dm^3/mol	ΔG_p, kJ/mol	K_b, dm^3/mol	ΔG_b, kJ/mol
$(HBE)_2Ni$	3920	–20.510	110.0	–11.65
$(BDM)_2Ni$	2490	–19.376	12.50	–9.81
$(BHBED)_2Ni$	13400	–23.550	6.67	–4.71
$(BDM)_2Zn$	1950	–18.770	31.40	–8.54
$(BHBED)_2Zn$	11.3	–6.010	125.00	–11.96
$(HBE)_2Co$	332	–24.330	476.00	–15.22

of complexes in the peripheral region of SDS micelles. The change in adsorption of metal complexes upon their binding with the surfactant micelles helped to calculate the binding and partition constants (K_b and K_x) [15–19].

Comparative interaction of selected metal complexes with SDS. UV-Vis spectroscopy and electrical conductivity data demonstrated the close agreement with the CMC in all cases. The highest partitioning constant (13400 dm^3/mol) of $(BHBED)_2Ni$/SDS system among all other complexes indicated its highest extent of partitioning between aqueous and micellar medium. On the contrary, the binding constant of $(HBE)_2Co$/SDS system (476 dm^3/mol) indicated its lowest partitioning tendency. Therefore, $(BHBED)_2Ni$ complex molecules were positioned near the peripheral region of micelles, while all other complexes were distributed in the other areas of micelles. The highest negative value ΔG_p (–24.33 kJ/mol) of $(BHBED)_2Ni$/SDS system exhibited its stability and spontaneity of the process. Position of the solubilizates in the micelles was determined by the partitioning coefficient, the greater value indicated their location in the outer region of the micelle and the molecule having the lowest value concentrated close to the core region (Scheme 2).

EXPERIMENTAL

All chemicals were purchased from the authorized chemical suppliers and used without additional purification. Elemental analysis was carried out on a Perkin-Elmer elemental analyzer. FTIR spectra were recorded on a Bio-Rad Merlin spectrophotometer in KBr disc. ^{1}H and ^{13}C NMR spectra were measured on a Bruker AM-250 spectrometers using $CDCl_3$ as a solvent and TMS as an internal reference. UV-Vis absorption was recorded on a Perkin-Elmer Lambda-25 spectrophotometer [32,33]. The absorbance of biological assays was recorded on a Synergy HT microplate reader.

Synthesis of ligands L1–L3. The equimolar amounts of *o*-phenylenediamine and carboxylic acids (**C1–C3**) were ground with a pestle in a mortar at room temperature

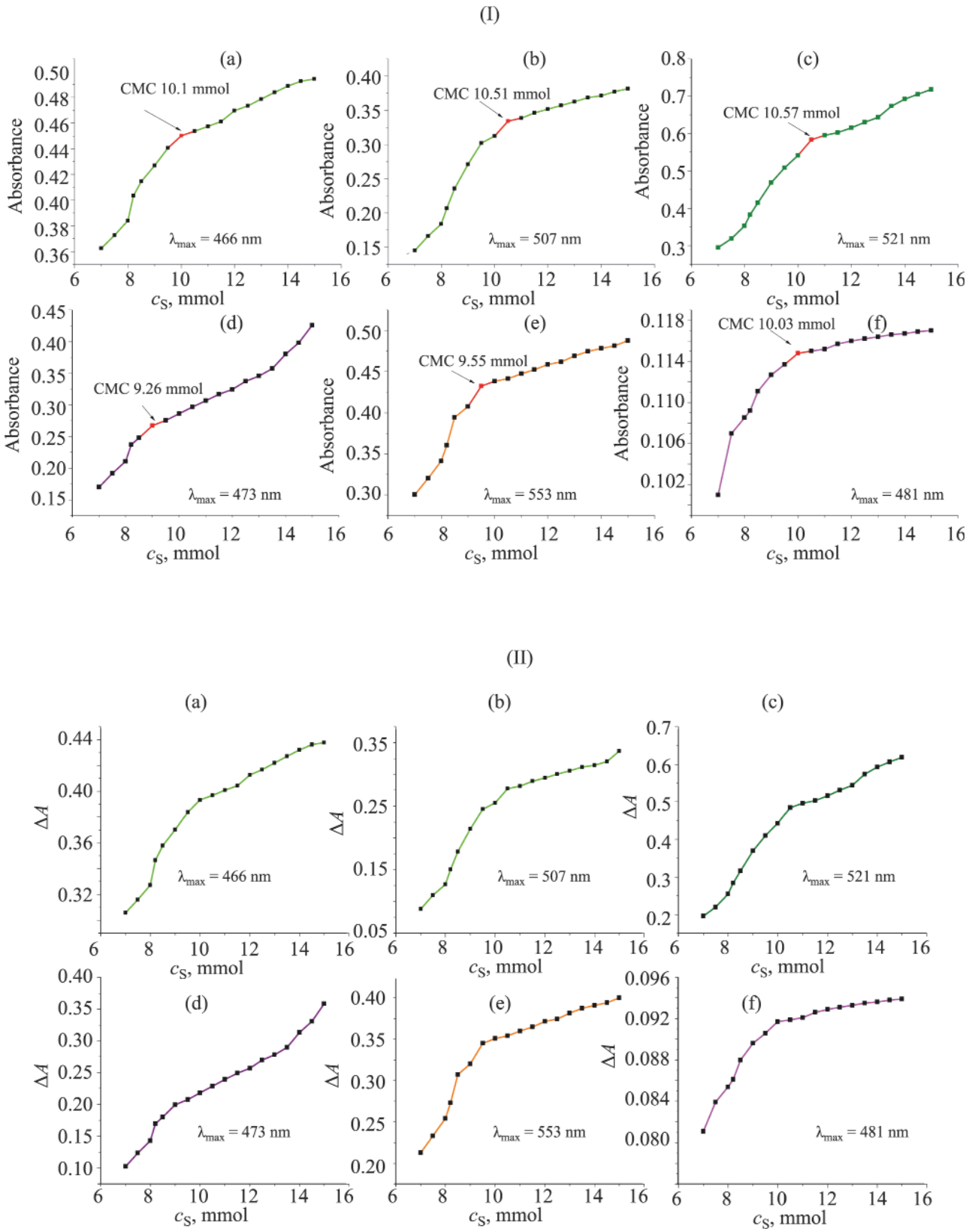

Fig. 2. UV-Vis absorbance of selected metal complexes in SDS. (I) Simple absorbance and (II) differntial absorbance; (a) $(HBE)_2Ni$, (b) $(BDM)_2Ni$, (c) $(BHBED)_2Ni$, (d) $(BDM)_2Zn$, (e) $(BHBED)_2Zn$, and (f) $(HBE)_2Co$.

Scheme 2.

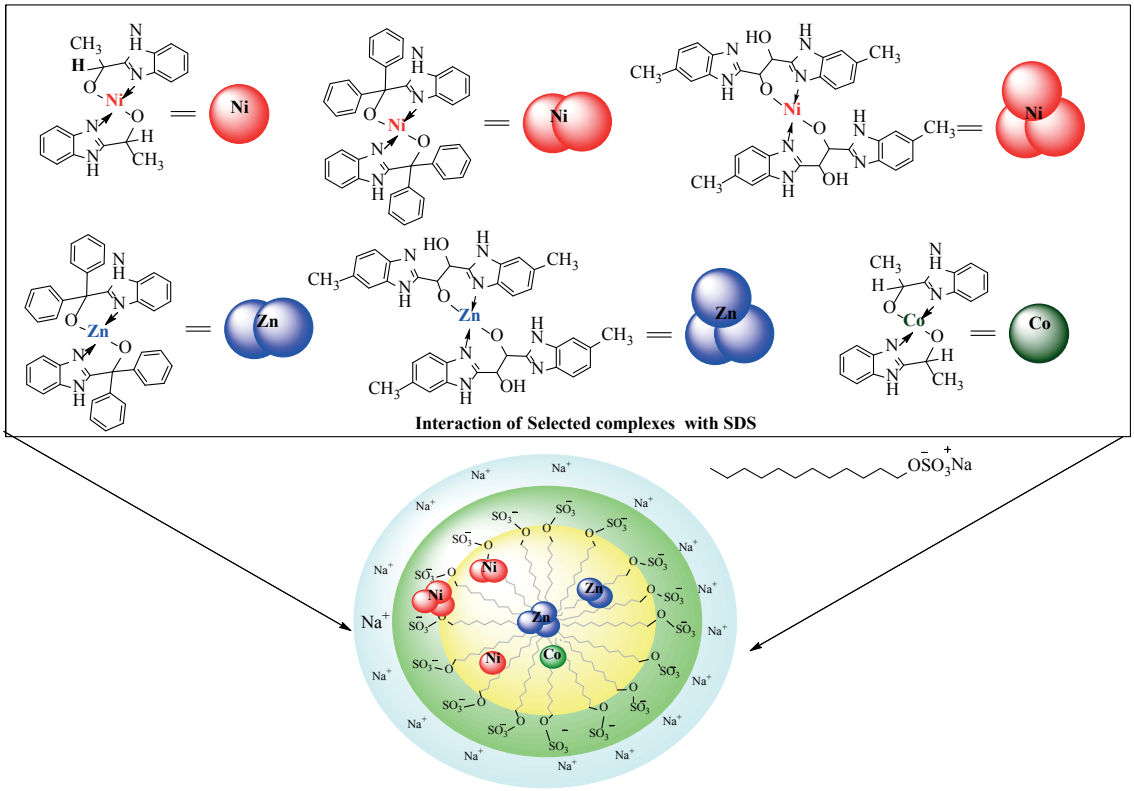

until the mixture melt. The molten mixture was heated at 140°C for ca. 1–2 h. Formation of ligands was monitored by TLC. Upon completion of the reaction, the molten mixtures were washed, and the products were purified in cold water.

1-(1*H*-Benzimidazol-2-yl)ethanol (L1). White amorphous solid, yield 65%, mp 184–186°C, R_f 0.7 (50% EtOAc–hexane). IR spectrum, ν, cm^{-1}: 3400 (N–H), 3235 (O–H), 1655 (C=N). ^1H NMR spectrum, δ, ppm: 4.3 (O–H), 6.9–7.5 (phenyl), 10.7 (N–H). ^{13}C NMR spectrum, δ_C, ppm: 25, 70, 120, 135, 156. Found, %: C 64.92; H 6.01; N 16.92, $C_9H_{10}N_2O$. Calculated, %: C 66.65; H 6.21; N 17.27. MS: *m/z*: 162 $[M]^+$.

1*H*-Benzimidazol-2-yl(diphenyl)methanol (L2). Light blue amorphous solid, yield 83%, mp 210–211°C, R_f 0.8 (50% EtOAc–hexane). IR spectrum, ν, cm^{-1}: 3410 (N–H), 3250 (O–H), 1645 (C=N). ^1H NMR spectrum, δ, ppm: 4.6 (N–H), 5.2 (O–H), 6.9–7.6 (phenyl). ^{13}C NMR spectrum, δ_C, ppm: 102, 118, 119, 124, 135, 142, 147. Found, %: C, 80.01; H, 5.30; N, 9.50. $C_{20}H_{16}N_2O$. Calculated, %: C 79.98; H 5.37; N 9.33. MS: *m/z*: 300 $[M]^+$.

1,2-Bis(1*H*-Benzimidazol-2-yl)ethane-1,2-diol (L3). Grey amorphous solid, yield 75 %, mp 189–191°C, R_f 0.8 (30% EtOAc–hexane). IR spectrum, ν, cm^{-1}: 3470 (N–H), 3050 (O–H), 1658 (C=N). ^1H NMR spectrum, δ, ppm: 2.9 (CH_3), 5.1 (O–H), 6.9–7.0 (phenyl), 8.84 (N–H). ^{13}C NMR spectrum, δ_C, ppm: 25, 71, 100, 110, 118, 126, 128, 138, 149, 154. Found, %: C 66.40; 5.79; N 17.10. $C_{18}H_{18}N_4O_2$. Calculated, % C 67.07; H 5.63; N17.38. MS: *m/z*: 322 $[M]^+$.

Synthesis of metals complexes. The mixture of 25 mL of aqueous solution of a synthesized ligand (**L1**–**L2**–**L3**, 1 equiv) with 25 mL of an aqueous solution of a metal salt (Cu^{2+}–Mn^{2+}–Zn^{2+}–Fe^{2+}–Co^{2+}–Ni^{2+}; 2 equiv) was heated in Teflon lined stainless steel autoclave at 100°C. Upon completion of the process, the product was filtered off, washed with distilled water and purified by ethanol. It was impossible to produce crystals appropriate for X-ray analysis.

$(HBE)_2Cu$ (1a). Light grey solid, yield 78%, mp 245–247°C. IR spectrum, ν, cm^{-1}: 3300 (N–H), 1660 (C=N). Found, %: C 57.10; H 4.40; N 13.45. $C_{18}H_{18}N_4O_2Cu$. Calculated, %: C 56.02; H 4.70; N 14.52.

$(HBE)_2Mn$ (1b). Off white solid, yield 70%, mp 235–236°C. IR spectrum, ν, cm^{-1}: 3330 (N–H), 1662 (C=N). Found, %: C 58.36; H 5.10; N 13.92. $C_{18}H_{18}N_4O_2Mn$. Calculated, %: C 57.30; H 4.81; N 14.85.

$(HBE)_2Zn$ (1c). White solid, yield 65%, mp 225–227°C. IR spectrum, ν, cm^{-1}: 3300 (N–H), 1665 (C=N). ^1H NMR spectrum, δ, ppm: 7.5–8.9 (phenyl), 9.3 (N–H). ^{13}C NMR spectrum, δ_C, ppm: 20, 65, 121, 125, 139, 156. Found, %: C 56.85; H 4.98; N 13.80. $C_{18}H_{18}N_4O_2Zn$. Calculated, %: C 55.76; H 4.68; N 14.45.

$(HBE)_2Fe$(1d). Brownish black solid, yield 54%, mp 250–253°C. IR spectrum, ν, cm^{-1}: 3310 (N–H), 1657 (C=N). Found, %: C 58.22; H 4.48; N 14.70. $C_{18}H_{18}N_4O_2Fe$. Calculated, %: C 57.16; H 4.80; N 14.81.

$(HBE)_2Co$ (1e). Light pink solid, yield 59%, mp 241–243°C. IR spectrum, ν, cm^{-1}: 3340 (N–H), 1665 (C=N). Found, %: C 56.60; H 4.50; N 14.80. $C_{18}H_{18}N_4O_2Co$. Calculated, %: C 56.70; H 4.76; N 14.69.

$(HBE)_2Ni$ (1f). Green solid, yield 70%, mp 209-210°C. IR spectrum, ν, cm^{-1}: 3352 (N–H), 1658 (C=N). ^1H NMR spectrum, δ, ppm: 6.5–6.9 (phenyl), 10.45 (N–H). ^{13}C NMR spectrum, δ_C, ppm: 23.4, 72, 127, 136, 145, 147. Found, %: C 57.20; H 5.20; N 13.95. $C_{18}H_{18}N_4O_2Ni$. Calculated, %: C 56.74; H 4.76; N 14.70.

$(BDM)_2Cu$ (2a). Greyish black solid, yield 70%, mp 255–257°C, R_f 0.9 (50% EtOAc–hexane). IR spectrum, ν, cm^{-1}: 3351 (N–H), 1650 (C–N). Found, %: C 72.55; H 4.55; N 8.41. $C_{40}H_{30}N_4O_2Cu$. Calculated, %: C 72.60; H 4.57; N 8.46.

$(BDM)_2Mn$ (2b). Off white solid, yield 65%, mp 217–220°C, R_f 0.6 (50% EtOAc–hexane). IR spectrum, ν, cm^{-1}: 3370 (N–H), 1657 (C–N). Found, %: C 72.40; H 4.64; N 8.55. $C_{40}H_{30}N_4O_2Mn$. Calculated, %: C 72.55; H 4.57; N 8.46.

$(BDM)_2Zn$ (2c). White solid, yield 73%, mp 230–232°C, R_f 0.85 (50% EtOAc–hexane). IR spectrum, ν, cm^{-1}: 3345 (N–H), 1652 (C=N). ^1H NMR spectrum, δ, ppm: 7.5–8.7 (phenyl), 9.9 (N–H). ^{13}C NMR spectrum, δ_C, ppm: 23, 83, 117, 124, 127, 138, 158. Found, %: C 72.24; H 4.50; N 8.65. $C_{40}H_{30}N_4O_2Zn$. Calculated, %: C 72.35; H 4.55; N 8.44.

$(BDM)_2Fe$ (2d). Pink solid, yield 60%, mp 236–238°C, R_f 0.62 (50% EtOAc–hexane). IR spectrum, ν, cm^{-1}: 3353 (N–H), 1660 (C–N). Found, %: C 73.42; H 4.44; N 8.77. $C_{40}H_{30}N_4O_2Fe$. Calculated, %: C 73.40; H 4.62; N 8.56.

$(BDM)_2Co$ (2e). Orange solid, yield 71%, mp 247–248°C, R_f 0.58 (50% EtOAc–hexane). IR spectrum, ν, cm^{-1}: 3362 (N–H), 1633 (C–N). Found, %: C 73.18; H 4.73; N 8.60. $C_{40}H_{30}N_4O_2Co$. Calculated, %: C 73. 06; H 4.60; N 8.52.

$(BDM)_2Ni$ (2f). Green solid, yield 76%, mp 245–247°C, R_f 0.8 (50% EtOAc–hexane). IR spectrum, ν, cm^{-1}: 3357 (N–H), 1659 (C=N). ^1H NMR spectrum, δ, ppm: 7.5–7.9 (phenyl), 8.3 (N–H). ^{13}C NMR spectrum, δ_C, ppm: 92, 113, 117, 128, 135, 146, 157. Found, %: C 68.12; H 4.39; N 7.51. $C_{40}H_{30}N_4O_2Ni$. Calculated, %: C 67.09; H 4.22; N 7.82.

$(BHBED)_2Cu$ (3a). Bluish green solid, yield 75%, mp 221–223°C, R_f 0.7 (50% EtOAc–hexane). IR spectrum, ν, cm^{-1}: 3347 (N–H), 1645 (C–N). Found, %: C 60.15; H 4.81; N 16.01. $C_{36}H_{34}N_8O_4Cu$. Calculated, %: C 61.22; H 4.85; N 15.87.

$(BHBED)_2Mn$ (3b). Light pink, yield 69%, mp 220–223°C, R_f 0.73 (50% EtOAc–hexane). IR spectrum, ν, cm^{-1}: 3353 (N–H), 1665 (C–N). Found, %: C 61.50; H 4.99; N 16.45. $C_{36}H_{34}N_8O_4Mn$. Calculated, %: C 61.98; H 4.91; N 16.06.

$(BHBED)_2Zn$ (3c). White, yield 83%, mp 235–237°C, R_f 0.66 (50% EtOAc–hexane). IR spectrum, ν, cm^{-1}: 3360 (N–H), 1670 (C=N). ^1H NMR spectrum, δ, ppm: 2.9 (N–H), 6.1 (O–H), 7.1–7.9 (phenyl), 9.3 (N–H), 10.1 (N–H). ^{13}C NMR spectrum, δ_C, ppm: 25, 57, 68, 110, 123, 125, 129, 132, 136, 147, 159. Found, %: C 60.62; H 4.79; N 15.67. $C_{36}H_{34}N_8O_4Zn$. Calculated, %: C 61.06; H 4.84; N 15.82.

$(BHBED)_2Fe$ (3d). Dark red solid, yield 65%, mp 248–251°C, R_f 0.83 (50% EtOAc–hexane). IR spectrum, ν, cm^{-1}: 3349 (N–H), 1654 (C–N). Found, %: C 62.01; H 4.82; N 16.41. $C_{36}H_{34}N_8O_4Fe$. Calculated, %: C 61.90; H 4.91; N 16.04.

$(BHBED)_2Co$ (3e). Pink solid, yield 69%, mp 253–254°C, R_f 0.58 (50% EtOAc–hexane). IR spectrum, ν, cm^{-1}: 3348 (N–H), 1656 (C–N). Found, %: C 60.70; H 4.93; N 15.97. $C_{36}H_{34}N_8O_4Co$. Calculated, %: C 61.63; H 4.88; N 16.36.

$(BHBED)_2Ni$ (3f). Greenish black solid, yield 73%, mp 250–253°C, R_f 0.6 (50% EtOAc–hexane). IR spectrum, ν, cm^{-1}: 3343 (N–H), 1668 (C=N). ^1H NMR spectrum, δ, ppm: 2.6 (N–H), 6.3 (O–H), 6.8–8.1 (phenyl), 10.3 (N–H), 11.6 (N–H). ^{13}C NMR spectrum, δ_C, ppm: 23, 49, 56, 98, 112, 119, 126, 129, 134, 136, 138, 151, 156. Found, %: C 60.89; H 4.72; N 15.46. $C_{36}H_{34}N_8O_4Ni$. Calculated, %: C 61.63; H 4.88; N 15.97.

Biological evaluation of metal complexes. *DPPH antioxidant activity.* The appropriate amount of a compound was dissolved in the solvent (10 μL), and 90 μL of 100 μM methanolic DPPH solution were added

to make a final volume of 100 μL in 96-well plates. The mixtures were thoroughly mixed and incubated for 30 min at 37°C and their absorbance was determined at 517 nm on a microplate reader. L-Ascorbic acid and quercetin were used as the standard antioxidants [20, 21]. IC_{50} values were calculated using EZ-Fit5 Perrella Scientific Inc. Amherst US software.

Acetylcholinesterase (AChE) inhibition activity. Acetylcholinesterase inhibition was studied using a total of 100 μL of the reaction content, which contained 60 μL of sodium phosphate buffer (50 mM; pH 7.7). The reaction mixture ca 10 μL of the metal complex (0.5 mM per well) was mixed with 10 μL of enzyme. Absorbance was measured at 405 nm and then pre-incubated for 10 min at 37°C. The reaction was initiated with 10 μL of acetylthiocholine iodide (0.5 mM/well) and incubated for 15 min at 37°C. Post-incubation absorbance of the reaction mixture was recorded at 405 nm. Triplicate experiments were carried out with eserine (0.5 mM/well) used as a positive control [22–24].

Butyrylcholinesterase (BChE) inhibition activity. Butyrylcholinesterase (BChE) inhibition was studied using 100 μL of the reaction mixture, which contained 60 μL of sodium phosphate buffer (50 mM; pH 7.7). The reaction mixture (ca 10 μL of the metal complex, 0.5 mM per well) was mixed with 10 μL of enzyme BChE. Absorbance of the content was measured at 405 nm, and then it was pre-incubated at 37°C for 10 min. The reaction was initiated with 10 μL of butyrylthiocholine chloride (0.5 mM/well), followed by addition of 10μL DTNB and then incubated for 15 min at 37°C. Post-incubation absorbance was also measured at 405 nm. Triplicate experiments were performed with eserine (0.5 mM/well) used as a positive control, and the percent inhibition was calculated [24].

Lipoxygenase (LOX) inhibition activity. Lipoxygenase inhibition was studied by using 200 μL of the reaction mixture containing 150 μL of sodium phosphate buffer (100 mM; pH 8.0), 10 μL of the test complexes and 15 μL of purified lipoxygenase enzyme (600 units per well). Absorbance of the reaction content was measured at 234 nm, and it was incubated at 25 °C for 10 min, followed by addition of substrate solution (25 μL) to initiate the reaction. Absorbance was measured again after 6 min of incubation at 234 nm. The assay was performed in triplicate with baicalin used as a positive control. The percent inhibition of samples was calculated [25].

α-Glucosidase inhibition activity. 100 μL of the reaction mixture containing 70 μL of phosphate buffer (50 mM; pH 6 .8) was used in this assay. The enzyme (10 μL; 0.057 units) was added to 10 μL (0.5 mM) of the test sample and incubated at 37°C for ca 10 min. Absorbance was measured at 400 nm. The substrate "*p*-nitrophenyl glucopyranoside" (10 μL; 0.5 mM) was then transferred to the reaction mixture to activate the reaction. Acarbose was used as a positive control. After incubating the reaction mixture for 30 min at 37°C, its absorbance was measured again to calculate percent inhibition [26].

Anti-urease activity. The 85 μL of the reaction mixture was mixed with 10 μL of sodium phosphate buffer (pH 7.0), and it was added to 96-well plate. The sample solution (10 μL) and the enzyme solution (25 μL; 0.134 units) were added subsequently. The reaction mixture was pre-incubated for 5 min at 37°C, then 40 μL of urea stock solution (20 mM) was transferred into wells and incubated for an additional 10 min at the same temperature. Each well was loaded with 115 μL of freshly prepared phenol hypochlorite (45 μL phenol reagent mixed in 70 μL of alkali reagent). The reaction content was further incubated under the same conditions for 10 min, the colour and absorbance were measured at 625 nm. The urease inhibition was computed [27].

Solubilization of synthesized complexes in SDS. The micellar solubilization of metal complexes with SDS was studied in aqueous solutions of metal complexes in deionized water for their conductometric and spectroscopic measurements [28–31]. For initial screening, the metal complexes were divided into three groups in accordance with the nature of the corresponding ligands **1a**–**1f**, **2a**–**2f**, **3a**–**3f**.

Electrical conductivity. Electrical conductivity measurements were recorded on a Hanna-Cond HI-99301 (capacity 0.01–199.9 mS) equipped with a platinum black electrode to subside polarization. Calibration of the electrode was carried out with KCl_{aq} over a certain range of SDS concentration. Measurements of specific conductivities were accomplished at three different temperatures with 10°C increment (25–45°C). All measurements of electrical conductivity were carried out in pre-micellar to post-micellar surfactant concentrations (7–15 mmol; CMC of pure SDS at 25°C, 8.2 mmol) [15–19, 34, 35]. Thermodynamic and other micellar parameters were derived from electrical conductivity data.

UV-Vis spectra. In the first step, aqueous primary solutions of metal complexes were prepared and then their secondary solutions were prepared by dissolving SDS in pre-micellar, micellar and post-micellar systems (7–15 mmol). The stock solutions were diluted by the serial dilution method ensuring applicability of the Lambert-Beer law to keep absorbance below 1. Simple absorbance was recorded using distilled water as a reference, whereas the differential absorbance was measured for an aqueous solution of SDS in a reference cell. The solutions of metal complexes with an aqueous solution of SDS (8.2 mmol; CMC of SDS) were loaded in the sample cell. The interactions were studied with the help of simple and differential absorbances, recorded in quartz cells (10 mm thick with a slit width of 1 nm) at 25°C (Fig 2). The extent of distribution of the metal complexes from aqueous to the micellar medium was evaluated from the partition coefficient as devised by the Kawamura model [36] which allowed to calculated experimental values of these solubilization parameters (Table 3).

CONCLUSIONS

One-pot efficient green synthesis of benzimidazole ligands and 3*d* transition metals complexes is worked out without any catalysts. This is the first report of the series of complexes with these benzimidazole ligands (HBE–BDM–BHBED) using the hydrothermal treatment. The biological properties and solubilization of the metal complexes with an anionic surfactant have been studied. The thermodynamic parameters including free energy, enthalpy and entropy of micellization have been determined by electrical conductivity. The interaction of metal complexes with sodium dodecyl sulphate (SDS) has been studied by UV-Vis spectroscopy and electrical conductivity. Such micellar interactions of 3*d* metals complexes with benzimidazole derivatives have been studied for the first time. Partition and binding constants, and their corresponding free energies have been studied by simple and differential UV-Vis spectroscopy. The values of CMC obtained spectrometrically and conductometrically are in close agreement.

ACKNOWLEDGMENTS

Authors gratefully acknowledge contributions from the Department of Chemistry, The Islamia University Bahawalpur and the Department of Chemistry, University of Agriculture, Faisalabad.

CONFLICT OF INTEREST

No conflict of interest was declared by the authors.

REFERENCES

1. Saify, Z.S., Kamil, A., Akhtar, S, Taha, M., Khan, A., Khan, K.M., Jahan, S., Rahim, F., Perveen, S., and Choudhary, M.I., *Med. Chem. Res.,* 2014, vol. 23, p. 4447. https://doi.org/10.1007/s00044-014-1015-z
2. Shaker, S.A., Khaledi, H., Cheah, S.-C., and Ali, H.M., *Arab. J. Chem.,* 2016, vol. 9, p. S1943. https://doi.org/10.1016/j.arabjc.2012.06.013
3. Liaqat, M., Mahmud, T., Hameed, A., Ashraf, M., Shafiq, M., and Asghar, H., *Inorg. Nano-Met. Chem.*, 2017, vol. 47, p. 1418. https://doi.org/10.1080/24701556.2017.1322613
4. Galal, S.A., Hegab, K.H., Kassab, A.S., Rodriguez, M.L., Kerwin, S.M., Abdel-Mo'men, A., and El Diwani, H.I., *Europ. J. Med. Chem.*, 2009, vol. 44, p.1500. https://doi.org/10.1016/j.ejmech.2008.07.013
5. Wang, H.-B., and Huang, J.-M. *Adv. Syn. Catal.,* 2016, vol. 358, p. 1975. https://doi.org/10.1002/adsc.201501167
6. Kovvuri, J., Nagaraju, B., Kamal, A., and Srivastava, A.K., *ACS Comb. Sci.,* 2016, vol. 18, p. 644. https://doi.org/10.1021/acscombsci.6b00107
7. Zhang, Z.-H., Yin, L., and Wang, Y.-M., *Cat. Comm.*, 2007, vol. 8, p. 1126. https://doi.org/10.1016/j.catcom.2006.10.022
8. Chen, C. and Chen, Y.J., *Tetrahedron Lett.,* 2004, vol. 45, p. 113. https://doi.org/10.1016/j.tetlet.2003.10.095
9. Ahmad, S. Taj, M.B., Tirmizi, S. A., Alelwani, W., Hajjar, D., Makki, A., Shah, S., Ali, U., Hassan, U., and Tahir, M., *Russ. J. Gen. Chem.,* 2019, vol. 89, p. 142. https://doi.org/10.1134/S1070363219010250
10. Amato, M., Caponetti, E., Martino, D.C., and Pedone, L., *J. Phys. Chem. B*, 2003, vol. 107, p. 10048. https://doi.org/10.1021/jp022697b
11. Usman, M., and Siddiq, M., *Spectrochim. Acta. A*, 2013, vol. 113, p. 182. https://doi.org/10.1016/j.saa.2013.04.089
12. Taboada, P., Ruso, J.M., Garcia, M., and Mosquera, V.C., *Colloids Surf. A*, 2001, vol. 179, p. 125. https://doi.org/10.1016/S0927-7757(00)00730-5
13. Usman, M. and Siddiq, M., *J. Chem. Therm.,* 2013, vol. 58, p. 359. https://doi.org/10.1016/j.jct.2012.11.022
14. Saeed, R., Usman, M., Mansha, A., Rasool, N., Naqvi, S.A.R., Zahoor, A.F., Rahman, H.M.A., Rana, U.A., and Al-Zahrani, E., *Colloids Surf. A*, 2017, vol. 512, p. 51. https://doi.org/10.1016/j.colsurfa.2016.10.016

15. Noor, S. and Rashid, M.A., *Tenside Surf. Deter.*, 2019, vol. 56, p. 490. https://doi.org/10.3139/113.110653
16. Noor, S., Younas, N., Rashid, M.A., Nazir, S., Usman, M., and Naz, T., *Colloid Interface Sci. Commun.*, 2018, vol. 27, p. 26. https://doi.org/10.1016/j.colcom.2018.09.004
17. Younas, N., Rashid, M.A., Usman, M., Nazir, S., Noor, S., Basit, A., and Jamil, M., *J. Surf. Det.*, 2017, vol. 20, p. 1311. https://doi.org/10.1007/s11743-017-1997-x
18. Younas, N., and Rashid, M.A., *Colloid Interface Sci. Commun.*, 2020, vol. 35, p. 100240. https://doi.org/10.1016/j.colcom.2020.100240
19. Younas, N., Rashid, M.A., Nazir, S., Usman, M., Sarfraz, R.A., Jamil, A., and Whitwood, A.C., *J. Mol. Liq*., 2017, vol. 240, p. 351. https://doi.org/10.1016/j.molliq.2017.05.052
20. Taha, M., Ismail, N.H., Jamil, W., Rashwan, H., Kashif, S.M., Sain, A.A., Adenan, M.I., Ali, M., Rahim, F., and Khan, K.M., *Eur. J. Med. Chem.*, 2014, vol. 84, p. 731. https://doi.org/10.1016/j.ejmech.2015.10.017
21. Ayhan-KIlcigİl, G., Kuş, C., Çoban, T., Can-Eke, B., Özbey, S., and Iscan, M., *J. Enzyme Inhib. Med. Chem*., 2005, vol. 20, p. 503. https://doi.org/10.1080/14756360500287086
22. Li, W., Li, W., Hu, Y., Xia, Y., Shen, Q., Nie, Z., Huang, Y., and Yao, S., *Biosens. Bioelectron.*, 2013, vol. 47, p. 345. https://doi.org/10.1016/j.bios.2013.03.038
23. Güngördü, A., Sireci, N., Küçükbay, H., Birhanli, A., and Ozmen, M., *Ecotoxicol. Environ. Saf.,* 2013, vol. 87, p. 23. https://doi.org/10.1016/j.ecoenv.2012.10.007
24. Yoon, Y.K., Ali, M.A., Wei, A.C., Choon, T.S., Khaw, K.Y., Murugaiyah, V., Osman, H., and Masand, V.H., *Bioorg. Chem.,* 2013, vol. 49, p. 33. https://doi.org/10.1016/j.bioorg.2013.06.008
25. Baylac, P.R., *Int. J. Aromather.,* 2003, vol. 13, p. 138. https://doi.org/10.1016/S0962-4562(03)00083-3
26. Zawawi, N.K.N.A. Taha, M., Ahmat, N., Wadood, A., Ismail, N.H., Rahim, F., Azam, S.S., and Abdullah, N., *Bioorg. Chem.,* 2016, vol. 64, p. 29. https://doi.org/10.1016/j.bioorg.2015.11.006
27. Karaali, N.J., *Turkish Chem. Soc.*, 2018, vol. 5, p. 971. https://doi.org/10.18596/jotcsa.440202
28. Usman, M., Cheema, M.A., Khan, A. Farooqi, Z.H., Mosquera, V., and Siddiq, M., *J. Chil. Chem. Soc.*, 2013, vol. 58, p. 1842. https://doi.org/10.4067/S0717-97072013000300010
29. Akhtar, F., Hoque, M.A., and Khan, M.A., *J. Chem. Thermodyn.,* 2008, vol. 40, p. 1082. https://doi.org/10.1016/j.jct.2008.03.001
30. Shah, A.M.K., Usman, M., Qureshi, R., Siddiq, M., and Shah, S.S., *J. Chil. Chem. Soc.,* 2009, vol. 54, p. 134. https://doi.org/10.4067/S0717-97072009000200007
31. Dani, D., Bahadur, A., and Kuperkar, K., *Colloid. Interface. Sci. Commun.*, 2015, vol. 25, p. 22. https://doi.org/10.1016/j.colcom.2018.06.002
32. Chari, M.A., Shobha, D., and Sasaki, T., *Tetrahedron Lett.*, 2011, vol. 52, p. 5575. https://doi.org/10.1016/j.tetlet.2011.08.047
33. Yan, Q., Zang, H., Wu, C., Feng, J., Li, M., Zhang, M., Wang, L., and Cheng, B., *J. Mol. Liq.,* 2015, vol. 204, p. 156. https://doi.org/10.1016/j.molliq.2015.01.016
34. Shedlovsky, T., *J. Am. Chem. Soc.,* 1932, vol. 54, p. 1411. https://doi.org/10.1021/ja01343a020
35. Chambers, J.F., Stokes, J.M., and Stokes, R.H., *J. Phys. Chem. A*, 1956, vol. 60, p. 985. https://doi.org/10.1021/j150541a040
36. Kawamura, H., Manabe, M., Miyamoto, Y., Fujita, Y., and Tokunaga, S., *J. Phys. Chem. A*, 1989, vol. 93, p. 5536. https://doi.org/10.1021/j100351a042